STAR-RIS Assisted Covert Communications in NOMA Systems

Han Xiao, *Student Member, IEEE,* Xiaoyan Hu*, *Member, IEEE,*
Yongxu Zhu, *Member, IEEE,* Tong-Xing Zheng, *Member, IEEE,* and Kai-Kit Wong, *Fellow, IEEE*

***Abstract*—Covert communications assisted by simultaneously transmitting and reflecting reconfigurable intelligent surface (STAR-RIS) in non-orthogonal multiple access (NOMA) systems have been explored in this paper. In particular, the access point (AP) transmitter adopts NOMA to serve a downlink covert user and a public user. The minimum detection error probability (DEP) at the warden is derived considering the uncertainty of its background noise, which is used as a covertness constraint. We aim at maximizing the covert rate of the system by jointly optimizing AP's transmit power and passive beamforming of STAR-RIS, under the covertness and quality of service (QoS) constraints. An iterative algorithm is proposed to effectively solve the non-convex optimization problem. Simulation results show that the proposed scheme significantly outperforms the conventional RIS-based scheme in ensuring system covert performance.**

***Index Terms*—Covert communications, STAR-RIS, NOMA.**

I. Introduction

The technology of covert communications (CCs) as a new security paradigm has attracted significant research interest in both civilian and military applications [1]. It can conceal the existence of communications between transceivers and provide a higher level of security for wireless communications than physical layer security. As a pioneer work, [2] first establishes the fundamental limit of CCs over additive white Gaussian noise (AWGN) channels from the perspective of information theory. Actually, the inherent unpredictability of wireless channels and the interference from other sources are ignored in [2], leading to a pessimistic solution. Later, [3], [4] demonstrate that more information bits can be covertly transmitted when eavesdroppers do not exactly know the power of background noise or channel state information (CSI).

The aforementioned works have validated the effectiveness of the CC techniques from different perspectives, however, they just investigate the simple CC scenarios with only one legitimate user served by a single-antenna AP transmitter. In order to expand to multi-user scenarios, multiple access techniques have to be adopted. Non-orthogonal multiple access (NOMA) is a promising technique that can achieve higher spectral efficiency, lower access delay, and massive connectivity than orthogonal multiple access (OMA) techniques [5]. Hence, NOMA holds significant potentials for wide-ranging applications in wireless communications and has been leveraged in CCs. For example, a covert NOMA communication scheme is proposed in [6], where the NOMA-weaker user transmits with random power to facilitate the covert transmissions between the covert user and the transmitter. In [7], authors explores the CCs of both the downlink and uplink transmissions in NOMA system.

While NOMA offers lots of advantages for communication systems, it is incapable of tackling the challenges posed by the randomness of wireless channels, which highly restrain the performance gains facilitated by NOMA. To desirably control the wireless propagation environment, the reconfigurable intelligent surface (RIS) and a more advanced RIS called simultaneously transmitting and reflecting RIS (STAR-RIS) have emerged as promising solutions which has been leveraged in many wireless communication scenarios including covert communications [8]–[10]. Unlike conventional RIS, STAR-RIS offers a more flexible full-space smart radio environment with 360° coverage, which can simultaneously control the coefficients of reflected and transmitted signals. This feature of STAR-RIS has drawn great attention from both academia and industry for its potential applications in wireless communications. However, the investigation of STAR-RIS aided wireless communication systems is still in its infancy stage. As for secure communications, only a small number of state-of-the-art works have utilized STAR-RISs to enhance the system secure performance with NOMA techniques [11], [12].

In this paper, we investigate the STAR-RIS assisted CC in NOMA systems to exploit its potential in enhancing the system covert performance. Specifically, we derive closed-form expressions for the minimum DEP and optimal detection threshold at the warden considering the worst-case scenario. We establish an optimization problem to maximize the covert rate under CC and quality of service (QoS) constraints by jointly optimizing the AP's transmit power allocation and the STAR-RIS's passive beamforming. The problem is non-convex and challenging to solve directly due to strong coupling among optimization variables. Hence, we propose an alternating optimization algorithm to solve it iteratively by addressing two subproblems: deriving the optimal power allocation in closed form with given passive beamforming and designing reflection and transmission coefficients effectively by the SDR method with given power allocation.

II. System Model

In this paper, we consider a STAR-RIS-assisted covert NOMA communication system, consisting of a single-antenna AP transmitter (Alice) aided by a STAR-RIS with M elements, a covert user (Bob), a public user (Carol) and a warden user (Willie) all equipped with a single antenna. We assume that the STAR-RIS is deployed at the users' vicinity to enhance the communications between Alice and legal users, i.e., Bob and Carol, which locate on opposite sides of the STAR-RIS and can be simultaneously served by the reflected (T) and transmitted (R) signals via STAR-RIS.

The wireless communication channels from Alice to STAR-RIS, and from STAR-RIS to Bob, Carol, Willie are represented as $\mathbf{h}_{\mathrm{AR}}=\sqrt{l_{\mathrm{AR}}}\mathbf{g}_{\mathrm{AR}}\in\ \mathbb{C}^{M\times 1}$, $\mathbf{h}_{\mathrm{rb}}=\sqrt{l_{\mathrm{rb}}}\mathbf{g}_{\mathrm{rb}}\in\ \mathbb{C}^{M\times 1}$, $\mathbf{h}_{\mathrm{rc}}=\sqrt{l_{\mathrm{rc}}}\mathbf{g}_{\mathrm{rc}}\in\mathbb{C}^{M\times 1}$ and $\mathbf{h}_{\mathrm{rw}}=\sqrt{l_{\mathrm{rw}}}\mathbf{g}_{\mathrm{rw}}\in\mathbb{C}^{M\times 1}$, respectively. Here, $\mathbf{g}_{\mathrm{AR}}$ and $\mathbf{g}_{\mathrm{rb}}$, $\mathbf{g}_{\mathrm{rc}}$, $\mathbf{g}_{\mathrm{rw}}$ are the small-scale Rayleigh

fading coefficients with independent identically distributed (i.i.d.) entries following complex Gaussian distribution with zero mean and unit variance. In addition, $l_{\rm AR}$ and $l_{\rm rb}$, $l_{\rm rc}$, $l_{\rm rw}$ are the large-scale path loss coefficients in the form of $\frac{\rho_0}{d^\alpha}$, where ρ_0 is the reference power gain at a distance of one meter (m), α indicates the path-loss exponent, and d represents to the node distances of $d_{\rm AR}$ and $d_{\rm rb}$, $d_{\rm rc}$, $d_{\rm rw}$. In this paper, we assume that the instantaneous CSI between STAR-RIS and Alice, Bob, Carol ($\mathbf{h}_{\rm AR}$, $\mathbf{h}_{\rm rb}$, $\mathbf{h}_{\rm rc}$) is available at Alice, while only the statistical CSI between STAR-RIS and Willie ($\mathbf{h}_{\rm rw}$) is known at Alice. In contrast, we consider the worst case that Willie is capable to know the global instantaneous CSI.

When Alice communicates with Bob and Carol, the received signals at Bob and Carol can be respectively expressed as

$$y_{\rm b}[k] = \mathbf{h}_{\rm rb}^H \mathbf{\Theta}_{\rm r} \mathbf{h}_{\rm AR} \big(\sqrt{P_{\rm b}} s_{\rm b}[k] + \sqrt{P_{\rm c}} s_{\rm c}[k]\big) + n_{\rm b}[k], \quad (1)$$

$$y_{\rm c}[k] = \mathbf{h}_{\rm rc}^H \mathbf{\Theta}_{\rm t} \mathbf{h}_{\rm AR} \big(\sqrt{P_{\rm b}} s_{\rm b}[k] + \sqrt{P_{\rm c}} s_{\rm c}[k]\big) + n_{\rm c}[k], \quad (2)$$

where $k \in \mathcal{K} \triangleq \{1, \ldots, K\}$ is the index of communication channel use in a time slot. $\mathbf{\Theta}_\chi = {\rm Diag}\left\{\sqrt{\beta_\chi^1} e^{{\rm j}\phi_\chi^1}, \ldots, \sqrt{\beta_\chi^M} e^{{\rm j}\phi_\chi^M}\right\}$ with $\chi \in \{{\rm r}, {\rm t}\}$ indicate the reflected and transmitted coefficient matrices of STAR-RIS, where $\beta_\chi^m \in [0,1]$, $\beta_{\rm r}^m + \beta_{\rm t}^m = 1$ and $\phi_\chi^m \in [0, 2\pi)$, for $\forall m \in \mathcal{M} \triangleq \{1, 2, \ldots, M\}$. In addition, $s_{\rm b}[k]$ and $s_{\rm c}[k] \sim \mathcal{CN}(0,1)$ are the covert and public signals transmitted by Alice to Bob and Carol with the power allocation $P_{\rm b}$ and $P_{\rm c}$, respectively. Here, $n_{\rm b}[k] \sim \mathcal{CN}(0, \sigma_{\rm b}^2)$ and $n_{\rm c}[k] \sim \mathcal{CN}(0, \sigma_{\rm c}^2)$ are the AWGN noise received at Bob and Carol with noise power $\sigma_{\rm b}^2$ and $\sigma_{\rm c}^2$.

III. Analysis on Covert Strategy

A. CC Detection Strategy at Willie

In this section, the detection strategy of Willie for covert communications from Alice to Bob is given in details. In fact, Willie faces a binary detection hypothesis based on the received signal sequence $\{y_{\rm w}[k]\}_{k\in\mathcal{K}}$, i.e., a null hypothesis $\mathcal{H}_0$ and an alternative hypothesis $\mathcal{H}_1$, respectively indicating that Alice only transmits public signals to Carol or both public and covert signals to Coral and Bob. Accordingly, the received signals at Willie for the two hypotheses are given by

$$\mathcal{H}_0 : y_{\rm w}[k] = \mathbf{h}_{\rm rw}^H \mathbf{\Theta}_{\rm r} \mathbf{h}_{\rm AR} \sqrt{P_{\rm c}} s_{\rm c}[k] + n_{\rm w}[k], \quad (3)$$

$$\mathcal{H}_1 : y_{\rm w}[k] = \mathbf{h}_{\rm rw}^H \mathbf{\Theta}_{\rm r} \mathbf{h}_{\rm AR} \big(\sqrt{P_{\rm b}} s_{\rm b}[k] + \sqrt{P_{\rm c}} s_{\rm c}[k]\big) + n_{\rm w}[k], \quad (4)$$

where $n_{\rm w}[k] \sim \mathcal{CN}(0, \sigma_{\rm w}^2)$ represents the background noise at Willie, which introduces the uncertainty to confuse Willie's detection for the covert communications. The probability density function (PDF) of the noise power $\sigma_{\rm w}^2$ is given as [3]

$$f_{\sigma_{\rm w}^2}(x) = \begin{cases} \frac{1}{2x \ln \rho}, & \frac{\hat{\sigma}_{\rm w}^2}{\rho} \le x \le \rho \hat{\sigma}_{\rm w}^2, \\ 0, & \text{otherwise}, \end{cases} \quad (5)$$

where $\rho > 1$ is the parameter that quantifies the size of the uncertainty, $\hat{\sigma}_{\rm w}^2$ represents the nominal noise power. Similar to [6], we assume that Willie utilizes a radiometer to detect covert transmissions, where the average power of the received signals in a time slot, i.e., $\overline{P}_{\rm w} = \frac{1}{K}\sum_{k=1}^K |y_{\rm w}[k]|^2$, is employed for statistical test. In addition, it is assumed that Willie takes infinite number of signal samples, i.e., $K \to \infty$, to implement binary detection [13], [14]. Therefore, the average received power $\overline{P}_{\rm w}$ can be asymptotically approximated as

$$\overline{P}_{\rm w} = \begin{cases} P_{\rm c} \left|\mathbf{h}_{\rm rw}^H \mathbf{\Theta}_{\rm r} \mathbf{h}_{\rm AR}\right|^2 + \sigma_{\rm w}^2, & \mathcal{H}_0, \\ (P_{\rm b} + P_{\rm c}) \left|\mathbf{h}_{\rm rw}^H \mathbf{\Theta}_{\rm r} \mathbf{h}_{\rm AR}\right|^2 + \sigma_{\rm w}^2, & \mathcal{H}_1. \end{cases} \quad (6)$$

Based on $\overline{P}_{\rm w}$, Willie makes the decision with the rule of $\overline{P}_{\rm w} \underset{\mathcal{D}_0}{\overset{\mathcal{D}_1}{\gtrless}} \tau_{\rm dt}$, where $\mathcal{D}_0$ or $\mathcal{D}_1$ indicates the decision that Willie favors the hypotheses of $\mathcal{H}_0$ or $\mathcal{H}_1$, and $\tau_{\rm dt} > 0$ is the detection threshold. Willie's detection performance is measured by the detection error probability (DEP) denoted as $P_{\rm e} \in [0,1]$, and we consider the worst case that Willie can optimize its detection threshold $\tau_{\rm dt}$ to minimize the DEP. It is known that the DEP $P_{\rm e}$ is the sum of the false alarm (FA) probability $P_{\rm FA} = \Pr(\mathcal{D}_1 \mid \mathcal{H}_0)$ and the miss detection (MD) probability $P_{\rm MD} = \Pr(\mathcal{D}_0 \mid \mathcal{H}_1)$ which respectively represent the probabilities of Willie making the decision $\mathcal{D}_1$ under $\mathcal{H}_0$ or $\mathcal{D}_0$ under $\mathcal{H}_1$. Hence, we can derive the DEP as

$$\begin{aligned} P_{\rm e} =& P_{\rm FA} + P_{\rm MD} \\ =& \Pr\left(\overline{P}_{\rm w} > \tau_{\rm dt} | \mathcal{H}_0\right) + \Pr\left(\overline{P}_{\rm w} < \tau_{\rm dt} | \mathcal{H}_1\right) \\ =& \Pr\left(\sigma_{\rm w}^2 > \tau_{\rm dt} - \phi_1\right) + \Pr\left(\sigma_{\rm w}^2 < \tau_{\rm dt} - \phi_2\right) \\ =& 1 - \Pr\left(\tau_{\rm dt} - \phi_2 \le \sigma_{\rm w}^2 \le \tau_{\rm dt} - \phi_1\right), \end{aligned} \quad (7)$$

where $\phi_1 = P_{\rm c} \left|\mathbf{h}_{\rm rw}^H \mathbf{\Theta}_{\rm r} \mathbf{h}_{\rm AR}\right|^2$, $\phi_2 = (P_{\rm b} + P_{\rm c}) \left|\mathbf{h}_{\rm rw}^H \mathbf{\Theta}_{\rm r} \mathbf{h}_{\rm AR}\right|^2$. It is assumed that the detection threshold $\tau_{\rm dt} \in \left[\frac{\hat{\sigma}_{\rm w}^2}{\rho} + \phi_1, \rho\hat{\sigma}_{\rm w}^2 + \phi_1\right]$ so that the uncertainty of the background noise at Willie can be fully used to explore its effect on the detection ability. Based on this assumption and the PDF of noise power at Willie, the analytical expression of $P_{\rm e}$ is given by

$$\begin{aligned} P_{\rm e} =& 1 - \int_{\max\left\{\tau_{\rm dt} - \phi_2, \frac{\hat{\sigma}_{\rm w}^2}{\rho}\right\}}^{\tau_{\rm dt} - \phi_1} \frac{1}{2x \ln \rho} dx = 1 - \frac{1}{2 \ln \rho} \times \\ & \left(\ln\left(\tau_{\rm dt} - \phi_1\right) - \ln\left(\max\left\{\tau_{\rm dt} - \phi_2, \frac{\hat{\sigma}_{\rm w}^2}{\rho}\right\}\right)\right). \end{aligned} \quad (8)$$

Theorem 1. *The closed-form optimal detection threshold $\tau_{\rm dt}^*$ to minimize the DEP at Willie in the considered STAR-RIS-assisted covert NOMA communication system is given as*

$$\tau_{\rm dt}^* = \min\left\{\phi_2 + \frac{\hat{\sigma}_{\rm w}^2}{\rho}, \phi_1 + \rho\hat{\sigma}_{\rm w}^2\right\}, \quad (9)$$

Proof: The proof is given in Appendix A. ∎

Substituting optimal detection threshold $\tau_{\rm dt}^*$ into (8) and adopting some algebraic manipulations, the analytical closed-form expression of the minimum DEP can be derived as

$$P_{\rm e}^* = \begin{cases} 1 - \frac{\ln\left(1 + \frac{\rho(\phi_2 - \phi_1)}{\hat{\sigma}_{\rm w}^2}\right)}{2 \ln \rho}, & \phi_2 - \phi_1 \le \frac{(\rho^2 - 1)\hat{\sigma}_{\rm w}^2}{\rho}, \\ 0, & \text{otherwise}. \end{cases} \quad (10)$$

In this paper, $\phi \triangleq \phi_2 - \phi_1 = P_{\rm b} \left|\mathbf{h}_{\rm rw}^H \mathbf{\Theta}_{\rm r} \mathbf{h}_{\rm AR}\right|^2 \le \frac{(\rho^2 - 1)\hat{\sigma}_{\rm w}^2}{\rho}$. To guarantee the covertness of communications between Alice and Bob, $P_{\rm e}^* \ge 1 - \epsilon$ is required, where $\epsilon \in (0,1)$ is determined by the system performance indicators. Based on this requirement, we can further obtain the constraint $\phi \le \min\left\{\frac{\left(\rho^{2\epsilon} - 1\right)\hat{\sigma}_{\rm w}^2}{\rho}, \frac{(\rho^2 - 1)\hat{\sigma}_{\rm w}^2}{\rho}\right\} = \frac{\left(\rho^{2\epsilon} - 1\right)\hat{\sigma}_{\rm w}^2}{\rho}$ to characterize the covert performance. Considering that Alice only possesses the

statistical CSI of $\mathbf{h}_{\rm rw}$, the average of ϕ over $\mathbf{h}_{\rm rw}$, denoted as $\overline{\phi} = \mathbb{E}(\phi)_{\mathbf{h}_{\rm rw}}$, is utilized to evaluate the covert communications between Alice and Bob. $\overline{\phi}$ can be expressed as $\overline{\phi} = \int_0^{+\infty} x \frac{e^{-\frac{x}{\lambda}}}{\lambda} dx = \lambda$, where $\lambda = P_{\rm b} l_{\rm rw} \left\| \mathbf{\Theta}_{\rm r} \mathbf{h}_{\rm AR} \right\|^2$. Therefore, the covert constraint can be given as $\lambda \leq \frac{1}{\rho} \left(\rho^{2\epsilon} - 1 \right) \hat{\sigma}_{\rm w}^2$.

B. Transmissions between Alice and Legitimate Users

In this paper, the legitimate users' CSI is adopted to determine the successive interference cancelation (SIC) decoding order in NOMA systems, which is a straightforward way being widely used in existing literature [6], [7]. It is assumed that Carol is allocated with more transmit power than Bob, i.e., $P_{\rm c} \geq P_{\rm b}$, so that the higher power of Carol can help to hide the covert transmissions between Alice and Bob from the detection of Willie in practical applications. Hence, Bob first decodes $s_{\rm c}[k]$ and eliminates it from the received signals, and then decodes its own signal $s_{\rm b}[k]$. Hence, the available decoding rates at Bob for $s_{\rm b}$ and $s_{\rm c}$ are respectively expressed as

$$R_{\rm bc} = \log_2 \left(1 + \frac{P_{\rm c} \left| \mathbf{h}_{\rm rb}^H \mathbf{\Theta}_{\rm r} \mathbf{h}_{\rm AR} \right|^2}{P_{\rm b} \left| \mathbf{h}_{\rm rb}^H \mathbf{\Theta}_{\rm r} \mathbf{h}_{\rm AR} \right|^2 + \sigma_{\rm b}^2} \right), \tag{11}$$

$$R_{\rm bb} = \log_2 \left(1 + \frac{P_{\rm b} \left| \mathbf{h}_{\rm rb}^H \mathbf{\Theta}_{\rm r} \mathbf{h}_{\rm AR} \right|^2}{\sigma_{\rm b}^2} \right). \tag{12}$$

For Carol, $s_{\rm c}$ is directly decoded by treating $s_{\rm b}$ as interference, and the available rate is given by

$$R_{\rm cc} = \log_2 \left(1 + \frac{P_{\rm c} \left| \mathbf{h}_{\rm rc}^H \mathbf{\Theta}_{\rm t} \mathbf{h}_{\rm AR} \right|^2}{P_{\rm b} \left| \mathbf{h}_{\rm rc}^H \mathbf{\Theta}_{\rm t} \mathbf{h}_{\rm AR} \right|^2 + \sigma_{\rm c}^2} \right). \tag{13}$$

IV. Problem Formulation and Algorithm Design

A. Optimization Problem Formulation

This section formulates an optimization problem to maximize the covert rate between Alice and Bob while ensuring the QoS at Carol, which is given below

$$\begin{aligned}
\max_{P_{\rm b}, P_{\rm c}, \mathbf{\Theta}_{\rm r}, \mathbf{\Theta}_{\rm t}} \quad & R_{\rm bb}, \\
\text{s.t. } & P_{\rm b} + P_{\rm c} \leq P_{\rm tmax}, P_{\rm c} \geq P_{\rm b}, && \text{(14a)} \\
& R_{\rm bc} \geq R_{\rm cc}, && \text{(14b)} \\
& R_{\rm cc} \geq R^*, && \text{(14c)} \\
& \lambda \leq \frac{1}{\rho} \left(\rho^{2\epsilon} - 1 \right) \hat{\sigma}_{\rm w}^2, && \text{(14d)} \\
& \beta_{\rm r}^m + \beta_{\rm t}^m = 1, \phi_{\rm r}^m, \phi_{\rm t}^m \in [0, 2\pi), m \in \mathcal{M}, && \text{(14e)}
\end{aligned}$$

through jointly optimizing Alice's transmit power and STAR-RIS's passive beamforming variables, i.e., $P_{\rm b}$, $P_{\rm c}$, $\mathbf{\Theta}_{\rm r}$ and $\mathbf{\Theta}_{\rm t}$. Here, (14a) include the transmit power constraints with $P_{\rm tmax}$ being the maximum transmit power of Alice; (14b) is the constraint that guarantees the successful SIC at Bob; (14c) represents the QoS constraint for Carol; (14d) is an equivalent covert communication constraint of $P_{\rm e}^* \geq 1 - \epsilon$; (14e) shows the amplitude and phase shift constraints for STAR-RIS. Actually, it is challenging to solve the formulated optimization problem because of the strong coupling among the optimization variables. To tackle this issue, the alternating strategy is leveraged to design the optimization algorithm. Specifically, we divide the original problem into two subproblems where one subproblems is focused on power allocation for Bob and Carol, i.e., $P_{\rm b}$, $P_{\rm c}$, while the other subproblem designs the passive beamformer variables $\mathbf{\Theta}_{\rm r}$ and $\mathbf{\Theta}_{\rm t}$.

B. Power Allocation Design

In this section, the transmit power allocation for Bob and Carol are obtained by solving the original optimization problem (14) with the given passive beamforming variables $\mathbf{\Theta}_{\rm r}$ and $\mathbf{\Theta}_{\rm t}$. Specifically, the objective function turns into maximizing $P_{\rm b}$, and the corresponding subproblem can be formulated as

$$\begin{aligned}
\max_{P_{\rm b}, P_{\rm c}} \quad & P_{\rm b}, \\
& \text{s.t. (14a)} - \text{(14d)}. && \text{(15a)}
\end{aligned}$$

We first deal with the constraint (14b) and can obtain that $\sigma_{\rm c}^2 \left| \mathbf{h}_{\rm rb}^H \mathbf{\Theta}_{\rm r} \mathbf{h}_{\rm AR} \right|^2 \geq \sigma_{\rm b}^2 \left| \mathbf{h}_{\rm rc}^H \mathbf{\Theta}_{\rm t} \mathbf{h}_{\rm AR} \right|^2$, which is irrelevant with $P_{\rm b}$ and $P_{\rm c}$. Thus, constraint (14b) can be removed from the problem (15). Similarly, by equivalently transforming the QoS constraint (14c) and the covert constraint (14d), the optimization problem (15) can be simplified as

$$\begin{aligned}
\max_{P_{\rm b}, P_{\rm c}} \quad & P_{\rm b}, \\
\text{s.t. } & \text{(14a)}, && \text{(16a)} \\
& P_{\rm b} \leq \frac{P_{\rm c} \left| \mathbf{h}_{\rm rc}^H \mathbf{\Theta}_{\rm t} \mathbf{h}_{\rm AR} \right|^2}{\left(2^{R^*} - 1 \right) \left| \mathbf{h}_{\rm rc}^H \mathbf{\Theta}_{\rm t} \mathbf{h}_{\rm AR} \right|^2} - \frac{\sigma_{\rm c}^2}{\left| \mathbf{h}_{\rm rc}^H \mathbf{\Theta}_{\rm t} \mathbf{h}_{\rm AR} \right|^2}, && \text{(16b)} \\
& P_{\rm b} \leq \frac{\left(\rho^{2\epsilon} - 1 \right) \hat{\sigma}_{\rm w}^2}{\rho l_{\rm rw} \left\| \mathbf{\Theta}_{\rm r} \mathbf{h}_{\rm AR} \right\|^2}, && \text{(16c)}
\end{aligned}$$

which is a simple linear programming problem. It is easy to derive the optimal solution as $P_{\rm b}^* = \min \left\{ \frac{P_{\rm tmax}}{2}, \frac{\left(\rho^{2\epsilon} - 1 \right) \hat{\sigma}_{\rm w}^2}{\rho l_{\rm rw} \left\| \mathbf{\Theta}_{\rm r} \mathbf{h}_{\rm AR} \right\|^2}, \frac{P_{\rm tmax} \left| \mathbf{h}_{\rm rc}^H \mathbf{\Theta}_{\rm t} \mathbf{h}_{\rm AR} \right|^2 - \left(2^{R^*} - 1 \right) \sigma_{\rm c}^2}{2^{R^*} \left| \mathbf{h}_{\rm rc}^H \mathbf{\Theta}_{\rm t} \mathbf{h}_{\rm AR} \right|^2} \right\}$ and $P_{\rm c}^* = P_{\rm tmax} - P_{\rm b}^*$.

C. Joint Passive Beamforming Design for STAR-RIS

In this subsection, the passive reflecting and transmitting beamforming variables $\mathbf{\Theta}_{\rm r}$ and $\mathbf{\Theta}_{\rm t}$ of STAR-RIS are jointly designed by solving the optimization problem (14) with the acquired $P_{\rm b}$ and $P_{\rm c}$ in previous subsection. The corresponding subproblem can be expressed as

$$\begin{aligned}
\max_{\mathbf{\Theta}_{\rm r}, \mathbf{\Theta}_{\rm t}} \quad & R_{\rm bb}, \\
& \text{s.t. (14b), (14c), (14d), (14e)}. && \text{(17a)}
\end{aligned}$$

Note that constraint (14b) and (14c) are non-convex with respect to (w.r.t.) $\mathbf{\Theta}_{\rm r}$ and $\mathbf{\Theta}_{\rm t}$, which makes this problem difficult to be solved directly. To effectively tackle this issue, we resort to the semi-definite relaxation (SDR) method. Specifically, let $\mathbf{Q}_\chi = \boldsymbol{\vartheta}_\chi^* \boldsymbol{\vartheta}_\chi^T$, $\boldsymbol{\beta}_\chi = \left[\beta_\chi^1, \cdots, \beta_\chi^M \right]$, where $\boldsymbol{\vartheta}_\chi = \mathrm{diag}(\mathbf{\Theta}_\chi)$ with $\chi \in \{ \mathrm{r}, \mathrm{t} \}$. It is easy to verify that $\mathbf{h}_{\rm rb}^H \mathbf{\Theta}_{\rm r} \mathbf{h}_{\rm AR} = \boldsymbol{\vartheta}_{\rm r}^T \mathbf{H}_{\rm rb}^* \mathbf{h}_{\rm AR}$, $\mathbf{h}_{\rm rc}^H \mathbf{\Theta}_{\rm t} \mathbf{h}_{\rm AR} = \boldsymbol{\vartheta}_{\rm t}^T \mathbf{H}_{\rm rc}^* \mathbf{h}_{\rm AR}$ and $\left\| \mathbf{\Theta}_{\rm r} \mathbf{h}_{\rm AR} \right\|_2^2 = \boldsymbol{\beta}_{\rm r}^T \left(\mathbf{h}_{\rm AR} \circ \mathbf{h}_{\rm AR}^* \right)$, where $\mathbf{H}_{\rm rb} = \mathrm{Diag}(\mathbf{h}_{\rm rb})$, $\mathbf{H}_{\rm rc} = \mathrm{Diag}(\mathbf{h}_{\rm rc})$ and $\circ$ means Hadamard product. Hence, problem (17) can be equivalently transformed as

$$\begin{aligned}
\max_{\mathbf{Q}_{\rm r}, \mathbf{Q}_{\rm t}, \boldsymbol{\beta}_{\rm r}, \boldsymbol{\beta}_{\rm t}} \quad & \mathrm{Tr}(\mathbf{Q}_{\rm r} \mathbf{A}), \\
\text{s.t. } & \sigma_{\rm c}^2 \, \mathrm{Tr}(\mathbf{Q}_{\rm r} \mathbf{A}) \geq \sigma_{\rm b}^2 \, \mathrm{Tr}(\mathbf{Q}_{\rm t} \mathbf{B}), && \text{(18a)} \\
& P_{\rm c} \, \mathrm{Tr}(\mathbf{Q}_{\rm t} \mathbf{B}) \geq \left(2^{R^*} - 1 \right) \left(P_{\rm b} \, \mathrm{Tr}(\mathbf{Q}_{\rm t} \mathbf{B}) + \sigma_{\rm c}^2 \right), && \text{(18b)} \\
& \boldsymbol{\beta}_{\rm r}^T \left(\mathbf{h}_{\rm AR} \circ \mathbf{h}_{\rm AR}^* \right) \leq \frac{\left(\rho^{2\epsilon} - 1 \right) \hat{\sigma}_{\rm w}^2}{P_{\rm b} l_{\rm rw} \rho}, && \text{(18c)} \\
& \mathrm{diag}(\mathbf{Q}_{\rm r}) = \boldsymbol{\beta}_{\rm r}, \mathrm{diag}(\mathbf{Q}_{\rm t}) = \boldsymbol{\beta}_{\rm t}, && \text{(18d)} \\
& \boldsymbol{\beta}_{\rm r} + \boldsymbol{\beta}_{\rm t} = \mathbf{I}_{M \times 1}, && \text{(18e)} \\
& \mathbf{Q}_{\rm r} \succeq 0, \mathbf{Q}_{\rm t} \succeq 0, && \text{(18f)} \\
& \mathrm{rank}(\mathbf{Q}_{\rm r}) = 1, \mathrm{rank}(\mathbf{Q}_{\rm t}) = 1, && \text{(18g)}
\end{aligned}$$

where $\mathbf{A} = \mathbf{H}_{\rm rb}^{*}\mathbf{h}_{\rm AR}\mathbf{h}_{\rm AR}^{H}\mathbf{H}_{\rm rb}^{T}$, $\mathbf{B} = \mathbf{H}_{\rm rc}^{*}\mathbf{h}_{\rm AR}\mathbf{h}_{\rm AR}^{H}\mathbf{H}_{\rm rc}^{T}$, However, problem (18) is still non-convex due to the two rank-one constraints in (18g). To solve this, we equivalently rewrite the rank-one constraints as [8]

$$\eta_{\chi} \triangleq {\rm Tr}(\mathbf{Q}_{\chi}) - \|\mathbf{Q}_{\chi}\|_2, \ \chi \in \{{\rm r}, {\rm t}\}, \tag{19}$$

where $\|\mathbf{Q}_{\chi}\|_2$ represents the spectral norm which is a convex function of $\mathbf{Q}_{\chi}$. Note that for any positive semi-definite matrix $\mathbf{Q} \succeq 0$, the inequality ${\rm Tr}(\mathbf{Q}) - \|\mathbf{Q}\|_2 \geq 0$ always holds and the equality is satisfied if and only if ${\rm rank}(\mathbf{Q}) = 1$. Based on the non-negative feature of $\eta_{\rm r}$ and $\eta_{\rm t}$, we add them into the objective function of problem (18) as penalty terms for the rank-one constraints. By replacing the convex spectral norms in $\eta_{\rm r}$ and $\eta_{\rm t}$ with their linear lower-bound, i.e., first-order Taylor expansions, we can obtain the upper-bound linear approximations for $\eta_{\rm r}$ and $\eta_{\rm t}$ as

$$\begin{aligned}\eta_{\chi} \leq & {\rm Tr}(\mathbf{Q}_{\chi}) - \left(\|\mathbf{Q}_{\chi}^{(i)}\|_2 + {\rm Tr}\left(\mathbf{q}_{\chi}^{(i)}(\mathbf{q}_{\chi}^{(i)})^{H}(\mathbf{Q}_{\chi} - \mathbf{Q}_{\chi}^{(i)})\right)\right) \\ = & \widehat{\eta}_{\chi}^{(i)}(\mathbf{Q}_{\chi}), \ \chi \in \{{\rm r}, {\rm t}\},\end{aligned} \tag{20}$$

where $\mathbf{q}_{\chi}^{(i)}$ is the eigenvectors corresponding to the largest eigenvalues of $\mathbf{Q}_{\chi}^{(i)}$ in i-th inner loop iteration. Thus, the optimization problem (18) can be re-expressed as

$$\begin{aligned}\max_{\mathbf{Q}_{\rm r}, \mathbf{Q}_{\rm t}, \boldsymbol{\beta}_{\rm r}, \boldsymbol{\beta}_{\rm t}} \ & {\rm Tr}(\mathbf{Q}_{\rm r}\mathbf{A}) - \xi_1\widehat{\eta}_{\rm r}^{(i)} - \xi_2\widehat{\eta}_{\rm t}^{(i)}, \\ {\rm s.t.} \ & ({\rm 18a}), ({\rm 18b}), ({\rm 18c}), ({\rm 18d}), ({\rm 18e}), ({\rm 18f}),\end{aligned} \tag{21a}$$

where $\xi_1 > 0$ and $\xi_2 > 0$ are the introduced penalty coefficients, which will iteratively increase to obtain the solutions that meet the rank-one constraint. As a result, optimization problem (21) is convex and can be effectively solved by existing convex optimization tools such as CVX [15].

D. Proposed Optimization Algorithm

Algorithm 1: Proposed Algorithm for Problem (14)

1: Initialize feasible point $\left(P_{\rm b}^{(0)}, P_{\rm c}^{(0)}, \boldsymbol{\Theta}_{\rm r}^{(0,0)}, \boldsymbol{\Theta}_{\rm t}^{(0,0)}\right)$; Define the tolerance accuracy ε and $\widehat{\varepsilon}$; Set the outer iteration index m = 0.
2: **While** $v > \varepsilon$ or $m = 0$ **do**
3: Solve the linear programming problem (15) and update $\left(P_{\rm b}^{(m+1)}, P_{\rm c}^{(m+1)}\right)$ with the obtained solutions.
4: Set inner iteration index i = 0; Initialize $\xi_1^{(0)}$ and $\xi_2^{(0)}$.
5: **While** $\widehat{v} > \widehat{\varepsilon}$ or $i = 0$ **do**
6: Solve problem (21) with given ($\boldsymbol{\Theta}_{\rm r}^{(m,i)}$, $\boldsymbol{\Theta}_{\rm t}^{(m,i)}$).
7: Update the ($\boldsymbol{\Theta}_{\rm r}^{(m,i+1)}$, $\boldsymbol{\Theta}_{\rm t}^{(m,i+1)}$) with the solution.
8: Calculate $\widehat{v} = \max\{\eta_{\rm r}, \eta_{\rm t}\}$ based on the acquired solution; Update the penalty coefficients $\xi_1^{(i+1)} = \omega\xi_1^{(i)}$, $\xi_2^{(i+1)} = \omega\xi_2^{(i)}$ and let $i = i + 1$.
9: **end while**
10: Update $\left(\boldsymbol{\Theta}_{\rm r}^{(m+1,0)}, \boldsymbol{\Theta}_{\rm t}^{(m+1,0)}\right)$ with $\left(\boldsymbol{\Theta}_{\rm r}^{(m,i)}, \boldsymbol{\Theta}_{\rm t}^{(m,i)}\right)$.
11: Calculate the objective value $R_{\rm bb}^{(m+1)}$ and update $v = \left|R_{\rm bb}^{(m+1)} - R_{\rm bb}^{(m)}\right|$; Let $m = m + 1$.
12: **end while**

The proposed iterative algorithm for effectively solving the initial optimization problem (14) is completed by Algorithm 1. This approach solves two subproblems in an alternating fashion, as elaborated in Section IV. Here, $v > 0$ represents the gap of objective function value between two adjacent iterations in outer loop and the algorithm will converge when v is below a predefined threshold ε. In addition, $\widehat{v} > 0$ denotes the penalty violation, $\omega > 1$ is the scaling factor of the penalty coefficient. For the proposed algorithm, the main computational complexity comes from solving the standard SDP subproblems in the second subproblem. For solving problem (21), the main complexity is dominated by $\mathcal{O}(2M^{3.5})$. which indicates that the complexity is mainly determined by the number of elements at STAR-RIS (M).

V. Simulation Results

In this section, the simulation results are presented to evaluate the covert performance of the proposed STAR-RIS assisted NOMA system. In particular, we set $\rho_0 = -20$ dB, $\alpha = 2$, and the distances $d_{\rm AR} = 100m$, $d_{\rm rb} = 20m$, $d_{\rm rc} = 15m$ and $d_{\rm rw} = 25m$. Further, we define $\rho = 3$ dB, the noise power $\sigma_{\rm b}^2 = -80$ dBm, $\sigma_{\rm c}^2 = -80$ dBm and $\hat{\sigma}_{\rm w}^2 = -80$ dBm. In the proposed algorithm, the tolerance parameters ε and $\widehat{\varepsilon}$ are set as 10^{-4} and 10^{-5}, respectively. In order to highlight the advantages of the proposed scheme, we consider a benchmark scheme with two conventional RIS each having $\frac{M}{2}$ elements to replace the STAR-RIS, where one RIS is the reflection-only RIS and the other is transmission-only RIS. We call this baseline scheme as "RIS-aided" scheme.

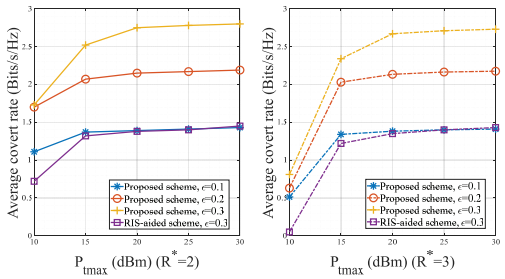

Fig. 1. Average covert rate versus the maximum transmit power $P_{\rm tmax}$.

Fig. 1 shows the influence of the maximum transmit power $P_{\rm tmax}$ on the average covert rate, considering $M = 40$ with different covert requirements ϵ and QoS constraints R^*. Specifically, the covert rate gradually increase with the growth of $P_{\rm tmax}$. In addition, we can find that the higher ϵ contributes to breaking the performance bottleneck imposed by channel characteristics and the number of elements at STAR-RIS. Compared with the RIS-aided baseline scheme, the proposed scheme possesses a strong superiority in enhancing the covert performance of the system even if tighter covert requirement is adopted. Further, lower covert rates are achieved in tighter QoS constraint (i.e., $R^* = 3$) and the degraded performance is the most obvious at $P_{\rm tmax} = 10$ dBm.

Next, we explore the performance of average covert rates versus covert requirement ϵ with different $P_{\rm tmax}$ and QoS requirements R^*, as presented in Fig. 2. We can observe that the covert rates have an upward trend with the increase of ϵ for all cases. To achieve an obvious comparison, $P_{\rm tmax} = 20$ dBm is selected to implement the RIS-aided baseline scheme,

while the acquired performance gain is still far below the proposed scheme even if the proposed scheme is operated at a lower power budget (i.e., $P_{\text{tmax}} = 15$ dBm). This is due to the STAR-RIS offers greater flexibility in reconfiguration as compared to conventional RIS, i.e., it can adjust the element phases and amplitudes for both reflection and transmission.

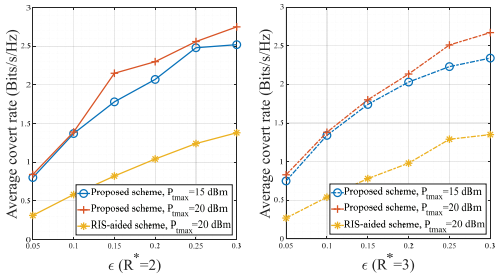

Fig. 2. Average covert rate versus covert requirement ϵ.

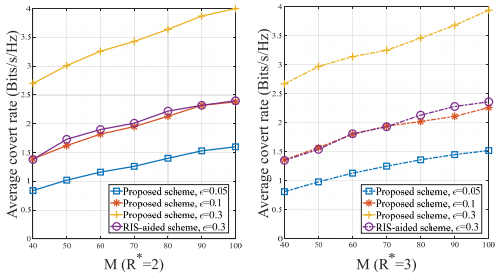

Fig. 3. Average covert rate versus the element number of STAR-RIS.

In Fig. 3, the variation curves of average covert rate w.r.t. the element number of STAR-RIS (M) are shown, under different ϵ and QoS constraints. It is observed that the average covert rates of all the schemes grow with M, since the increased elements can provide higher degrees of freedom for re-configuration of the propagation environment. The RIS-aided baseline scheme is operated with $\epsilon = 0.3$. Under the same covert requirement constraint, the proposed STAR-RIS-aided scheme outperforms the benchmark schemes, and the advantage becomes more significant as M increases.

VI. Conclusion

In this work, the STAR-RIS-assisted covert communication in NOMA system is investigated. We first derive the closed-form expression of the minimum DEP which is utilized to characterize the covert performance of the system. Then, an optimization problem maximizing the covert rate of the system under the covertness and QoS constraints is established by jointly optimizing the transmit power allocation and passive beamformer. Due to the strong coupling among optimization variables, an iterative algorithm is proposed to effectively solve this optimization problem. Simulation results demonstrate that the STAR-RIS-assisted covert communication scheme highly outperforms the conventional RIS-aided scheme.

Appendix A
Proof of Theorem 1

According to the derived expression of DEP in (8), we can see that P_{e} is a segment function of detection threshold τ_{dt}. Next, let us derive the optimal detection threshold τ_{dt}^*.

1) $\tau_{\text{dt}} \geq \phi_2 + \frac{\sigma_{\text{w}}^2}{\rho}$*:* It is easy to derive $P_{\text{e}} = 1 - \frac{1}{2\ln\rho}\ln\left(\frac{\tau_{\text{dt}}-\phi_1}{\tau_{\text{dt}}-\phi_2}\right)$. First, we calculate the first-order partial derivative of P_{e} w.r.t. τ_{dt}, which is expressed as

$$\frac{\partial P_{\text{e}}}{\partial \tau_{\text{dt}}} = \frac{1}{2\ln\rho}\left(\frac{1}{\tau_{\text{dt}}-\phi_2} - \frac{1}{\tau_{\text{dt}}-\phi_1}\right). \tag{22}$$

We can find that $\frac{\partial P_{\text{e}}}{\partial \tau_{\text{dt}}} > 0$ always holds. Hence, the optimal detection threshold in this range is $\tau_{\text{dt}}^* = \phi_2 + \frac{\sigma_{\text{w}}^2}{\rho}$.

2) $\tau_{\text{dt}} < \phi_2 + \frac{\sigma_{\text{w}}^2}{\rho}$*:* The P_{e} can be derived as $P_{\text{e}} = 1 - \frac{1}{2\ln\rho}\ln\left(\frac{\rho(\tau_{\text{dt}}-\phi_1)}{\hat{\sigma}_{\text{w}}^2}\right)$, and its first-order partial derivative w.r.t. τ_{dt} is given as $\frac{\partial P_{\text{e}}}{\partial \tau_{\text{dt}}} = -\frac{1}{2\ln\rho}\frac{1}{\tau_{\text{dt}}-\phi_1}$ where $\frac{\partial P_{\text{e}}}{\partial \tau_{\text{dt}}} < 0$ holds.

Base on above analysis and $\tau_{\text{dt}} \in \left[\frac{\hat{\sigma}_{\text{w}}^2}{\rho}+\phi_1, \rho\hat{\sigma}_{\text{w}}^2+\phi_1\right]$, the optimal detection threshold τ_{dt}^* can be derived as

$$\tau_{\text{dt}}^* = \min\left\{\phi_2 + \frac{\sigma_{\text{w}}^2}{\rho}, \phi_1 + \rho\hat{\sigma}_{\text{w}}^2\right\}. \tag{23}$$

References

[1] S. Yan, X. Zhou, J. Hu, and S. V. Hanly, "Low probability of detection communication: Opportunities and challenges," *IEEE Wireless Commun.*, vol. 26, no. 5, pp. 19–25, 2019.

[2] B. A. Bash, D. Goeckel, and D. Towsley, "Limits of reliable communication with low probability of detection on AWGN channels," *IEEE J. Sel. Areas Commun.*, vol. 31, no. 9, pp. 1921–1930, 2013.

[3] B. He, S. Yan, X. Zhou, and V. K. Lau, "On covert communication with noise uncertainty," *IEEE Commun. Lett.*, vol. 21, no. 4, pp. 941–944, 2017.

[4] J. Wang, W. Tang, Q. Zhu, X. Li, H. Rao, and S. Li, "Covert communication with the help of relay and channel uncertainty," *IEEE Wireless Commun. Lett.*, vol. 8, no. 1, pp. 317–320, 2018.

[5] Z. Ding, R. Schober, and H. V. Poor, "Unveiling the importance of SIC in NOMA systems Part 1: State of the art and recent findings," *IEEE Commun. Lett.*, vol. 24, no. 11, pp. 2373–2377, 2020.

[6] L. Tao, W. Yang, S. Yan, D. Wu, X. Guan, and D. Chen, "Covert communication in downlink NOMA systems with random transmit power," *IEEE Wireless Commun. Lett.*, vol. 9, no. 11, pp. 2000–2004, 2020.

[7] L. Lv, Q. Wu, Z. Li, Z. Ding, N. Al-Dhahir, and J. Chen, "Covert communication in intelligent reflecting surface-assisted NOMA systems: Design, analysis, and optimization," *IEEE Trans. Wireless Commun.*, vol. 21, no. 3, pp. 1735–1750, 2021.

[8] X. Hu, C. Masouros, and K.-K. Wong, "Reconfigurable intelligent surface aided mobile edge computing: From optimization-based to location-only learning-based solutions," *IEEE Trans. Commun.*, vol. 69, no. 6, pp. 3709–3725, 2021.

[9] Y. Liu, X. Mu, J. Xu, R. Schober, Y. Hao, H. V. Poor, and L. Hanzo, "STAR: Simultaneous transmission and reflection for 360° coverage by intelligent surfaces," *IEEE Wireless Commun.*, vol. 28, no. 6, pp. 102–109, 2021.

[10] H. Xiao, X. Hu, P. Mu, W. Wang, T.-X. Zheng, K.-K. Wong, and K. Yang, "Simultaneously transmitting and reflecting RIS (STAR-RIS) assisted multi-antenna covert communications: Analysis and optimization," *arXiv preprint arXiv:2305.04930*, 2023.

[11] Y. Han, N. Li, Y. Liu, T. Zhang, and X. Tao, "Artificial noise aided secure NOMA communications in STAR-RIS networks," *IEEE Wireless Commun. Lett.*, 2022.

[12] Z. Zhang, J. Chen, Y. Liu, Q. Wu, B. He, and L. Yang, "On the secrecy design of STAR-RIS assisted uplink NOMA networks," *IEEE Trans. Wireless Commun.*, vol. 21, no. 12, pp. 11 207–11 221, 2022.

[13] J. Hu, S. Yan, X. Zhou, F. Shu, and J. Li, "Covert wireless communications with channel inversion power control in rayleigh fading," *IEEE Trans. Veh. Technol.*, vol. 68, no. 12, pp. 12 135–12 149, 2019.

[14] C. Wang, Z. Li, J. Shi, and D. W. K. Ng, "Intelligent reflecting surface-assisted multi-antenna covert communications: Joint active and passive beamforming optimization," *IEEE Trans. Commun.*, vol. 69, no. 6, pp. 3984–4000, 2021.

[15] M. Grant and S. Boyd, "CVX: Matlab software for disciplined convex programming, version 2.1," 2014.